Published OnlineFirst August 8, 2014; DOI: 10.1158/1078-0432.CCR-13-3191

Cancer Therapy: Preclinical

Clinical Cancer Research

Overexpression of Smad7 Blocks Primary Tumor Growth and Lung Metastasis Development in Osteosarcoma

Audrey Lamora[1,2,3,4], Julie Talbot[1,2,3], Gwenola Bougras[1,2,3], Jérôme Amiaud[1,2,3], Marion Leduc[1,2,3], Julie Chesneau[1,2,3], Julien Taurelle[1,2,3], Verena Stresing[1,2,3], Marie Cécile Le Deley[5], Marie Françoise Heymann[1,2,3], Dominique Heymann[1,2,3], Françoise Redini[1,2,3], and Franck Verrecchia[1,2,3]

Abstract

Purpose: Osteosarcoma is the main malignant primary bone tumor in children and adolescents for whom the prognosis remains poor, especially when metastasis is present at diagnosis. Because transforming growth factor-β (TGFβ) has been shown to promote metastasis in many solid tumors, we investigated the effect of the natural TGFβ/Smad signaling inhibitor Smad7 and the TβRI inhibitor SD-208 on osteosarcoma behavior.

Experimental Design: By using a mouse model of osteosarcoma induced by paratibial injection of cells, we assessed the impact of Smad7 overexpression or SD-208 on tumor growth, tumor microenvironment, bone remodeling, and metastasis development.

Results: First, we demonstrated that TGFβ levels are higher in serum samples from patients with osteosarcoma compared with healthy volunteers and that TGFβ/Smad3 signaling pathway is activated in clinical samples. Second, we showed that Smad7 slows the growth of the primary tumor and increases mice survival. We furthermore demonstrated that Smad7 expression does not affect *in vitro* osteosarcoma cell proliferation but affects the microarchitectural parameters of bone. In addition, Smad7-osteosarcoma bone tumors expressed lower levels of osteolytic factors such as RANKL, suggesting that Smad7 overexpression affects the "vicious cycle" established between tumor cells and bone cells by its ability to decrease osteoclast activity. Finally, we showed that Smad7 overexpression in osteosarcoma cells and the treatment of mice with SD208 inhibit the development of lung metastasis.

Conclusion: Taken together, these results demonstrate that the inhibition of the TGFβ/Smad signaling pathway may be a promising therapeutic strategy against tumor progression of osteosarcoma, specifically against the development of lung metastasis. *Clin Cancer Res; 20(19); 5097–112. ©2014 AACR.*

Introduction

Osteosarcoma is the most common primary malignant bone tumor in children and adolescents with a second peak of incidence in adults over the age of 65 (1). Although several predisposing environmental (e.g., ionizing radiation) and genetic (e.g., *TP53*) factors have been identified (2), the exact etiology of this disease remains unknown (3). These rare tumors, believed to originate from mesenchymal cells forming the primitive bone, preferentially grow in the metaphysis of long bone (4). Approximately 20% of patients have lung metastasis at initial diagnosis and an additional 40% will develop metastasis during the later stages of disease. The presence of metastasis at diagnosis is the most important predictor of disease-free survival with a 5-year survival rate of only 20% for osteosarcoma patients with metastasis compared with 65% for patients with localized disease (5). The standard treatment of osteosarcoma consists of complete surgical resection associated with neoadjuvant and adjuvant chemotherapy composed of 4 agents: doxorubicin, cisplatin, methotrexate or ifosfamide (6). These combined treatment protocols have significantly improved survival of the nonmetastatic patients over the past several decades (7, 8). Unfortunately, such therapeutic strategies have a limited efficacy in the treatment of metastatic disease, and the metastatic relapse or recurrent conditions have remained unchanged over the last 3 decades (8). Treating metastatic osteosarcoma thus remains a challenge in bone cancer (9).

Transforming growth factor-β (TGFβ) family members are a class of cytokines that control a variety of biologic processes, including proliferation, differentiation, extracellular matrix production, and apoptosis. Three isoforms of TGFβ exist in mammals: TGFβ1, TGFβ2, and TGFβ3.

[1]INSERM, UMR 957, Equipe labellisée Ligue contre le Cancer 2012, Nantes, France. [2]Université de Nantes, Laboratoire de Physiopathologie de la Résorption Osseuse et Thérapie des Tumeurs Osseuses Primitives, Nantes, France. [3]CHU Hôtel Dieu, Nantes, France. [4]Inserm Liliane Bettencourt School, Paris, France. [5]Institut Gustave Roussy, Villejuif, France.

Note: Supplementary data for this article are available at Clinical Cancer Research Online (http://clincancerres.aacrjournals.org/).

Corresponding Author: Franck Verrecchia, INSERM, UMR 957, Faculté de Médecine, 1 rue Gaston Veil, 44000 Nantes, France. Phone: 33-240412842; Fax: 33-240412860; E-mail: franck.verrecchia@inserm.fr

doi: 10.1158/1078-0432.CCR-13-3191

Published OnlineFirst August 8, 2014; DOI: 10.1158/1078-0432.CCR-13-3191

Translational Relevance

We have demonstrated that the TGFβ/Smad signaling pathway plays a crucial role in osteosarcoma metastatic progression. We have first shown that TGFβ levels are higher in serum samples from patients with osteosarcoma compared with healthy volunteers and that the TGFβ/Smad3 signaling pathway is activated in clinical samples of patients. Second, using a murine model of osteosarcoma, we demonstrated that blocking the TGFβ/Smad signaling pathway via overexpression of inhibitory Smad slows the growth of the primary bone tumor mainly by affecting the tumor microenvironment by controlling the "vicious cycle" established between tumor cells and bone cells. Third, blocking TGFβ signaling inhibits the development of lung metastasis at least by inhibition of cell migration and invasion. Here, we show for the first time that blocking TGFβ signaling represents a novel therapeutic approach for the treatment of lung metastasis in patients with osteosarcoma, which has a poor prognosis.

Dimers of TGFβ initiate the canonical signaling cascade via the serine/threonine kinase receptor cell surface complexes (TβRI and TβRII), which phosphorylate the ligand-specific receptor-activated Smads (R-Smad: Smad2 or Smad3). Upon phosphorylation by type I receptors, R-Smads form a heteromeric complex with the Common-Smad, Smad4. The R-Smad/Smad4 complex then translocates to the nucleus to regulate gene transcription (10–13). A third group of Smad proteins, the inhibitory Smads (Smad7), inhibits the canonical Smad signaling (14, 15) by different means; Smad7 (i) binds TβRI and prevents R-Smad phosphorylation, (ii) recruits E3-type ubiquitin ligases to the receptor complexes ultimately leading to their degradation, and (iii) interacts with GADD34, the regulatory subunit of the protein phosphatase PP1 to inactive TβRI (10–16).

The role of TGFβ in cancer is complex. During the first stages of the development of primitive tumors from epithelial origin, the TGFβ/Smad cascade acts as a tumor suppressor mainly through inhibition of cell proliferation and/or promotion of cell apoptosis (11, 12, 17). Contrarily, during the later stages, the TGFβ cascade promotes tumor progression mainly by its ability to stimulate epithelial-to-mesenchymal transition, tumor invasion, metastatic dissemination, and/or evasion of the immune system (12, 13, 17). With regard to bone cancers, most studies have focused on the role of TGFβ in the development of bone metastasis. The contributions of TGFβ to breast cancer and melanoma bone metastasis have been well described (18–21). TGFβ promotes bone metastasis by its ability to promote the metastatic process by stimulating MMP2 production and thus promoting cellular invasion of melanoma (19, 20). It has been reported that TGFβ contributes to the establishment of a vicious cycle between epithelial tumor cells and bone cells. Briefly, the tumor cells secrete osteoclast-activating factors that promote bone degradation, thus stimulating the release of factors which in turn will promote bone metastasis development (22, 23). In this context, it has been shown that overexpression of the TGFβ inhibitor Smad7 in melanoma cells reduces the development of melanoma bone metastasis, and that the use of chemical inhibitors targeting TβRI reduces the development and progression of both melanoma and breast cancer bone metastasis (21). With regard to primary bone sarcomas, few studies have described the role of TGFβ on tumor development. It has been shown that the production of TGFβ1 is associated with high-grade osteosarcoma (24, 25) and that TGFβ stimulates the growth of several osteosarcoma cell lines in culture (26), suggesting that TGFβ could favor osteosarcoma development.

In this study, we particularly demonstrate that the overexpression of the inhibitory Smad, Smad7, in osteosarcoma cells and treatment of mice with a specific inhibitor of TβRI (SD-208) block the development of osteosarcoma lung metastasis.

Materials and Methods

Measurement of circulating TGFβ levels in serum

The levels of circulating TGFβs were measured in serum from healthy controls ($n = 20$) from the Etablissement Français du Sang (EFS) and patients with osteosarcoma ($n = 40$) from the OS 2006 protocol (PAC SARCOME, Sarcome 09/0603, EudraCT No. 2006-00337727) with the Bio-Plex Pro Assay TGFβ Standard 3-Plex system (Bio-Rad). Serum samples were obtained with written informed consent.

Cell cultures and reagents

HOS and SaOS2 osteosarcoma cells were purchased from ATCC (CRL-1544 and HTB-85, respectively) and cultured in Dulbecco's modified Eagle medium (DMEM; Lonza) supplemented with 10% fetal bovine serum (Hyclone Perbio). All cell lines were authenticated by short tandem repeat (STR) profiling. TGFβ1 and BMP-6, and G418 were, respectively, from R&D System Inc. and Sigma. SD-208 has been synthetized by the laboratory CEISAM UMR6230, Nantes University (France).

Western blot analysis

Western blot analysis were performed as previously described (27). Membranes were immunoblotted with anti–phospho-Smad3 (Millipore), anti-Smad3 (Millipore), anti-Smad7 (Santa Cruz Biotechnology), anti–phospho-Erk (Cell Signaling Technology), anti-Erk (Cell Signaling), or anti–β-actin (Sigma) antibodies.

Proliferation assay

Cell growth and viability were determined by using a 2,3-bis(2 methoxy-4 nitro-5-sulfophenyl)-2H-tetrazolium-5-carboxanilide (XTT) Reagent Assay Kit (Roche Molecular Biomedicals).

Published OnlineFirst August 8, 2014; DOI: 10.1158/1078-0432.CCR-13-3191

Table 1. Primer sequence for quantitative RT-PCR

	Sens	Antisens
ANGPTL4	gAC CCg gCT CAC AAT gTC	CCC TgA ggC Tgg ATT TCA
Col1A1	CTg gAC CTA Aag gTg cTg cT	gCT CCA gCC TCT CCA TCT TT
CTGF	CTC CTg Cag gCT AgA gAA gC	gAT gCA CTT TTT gCC CTT CTT
CXCR4	CCg Agg AAA Tgg gCT CAg ggg A	TgA Tgg AgT AgA Tgg Tgg gCA ggA
GAPDH	Tgg gTg TgA ACC Atg AgA AgT Atg	ggT gCA ggA ggC ATT gCT
ID1	AAT CAT gAA AgT CgC Cag Tg	ATg TCg Tag AgC AgC ACg TTT
IL11	gCA gCg gAC Agg gAA ggg TTA A	ACA ggC TCA gCA CgA CCA gg
MMP2	AgA Agg CTg TgT TCT TTg CAg	Agg CTg gTC AgT ggC TTg
OPN	gAg ggC TTg gTT gTC AgC	CAA TTC TCA Tgg Tag TgA gTT TTC C
PAI-1	Cag ACC Aag AgC CTC TCC AC	ATC ACT Tgg CCC Atg AAA Ag
RANKL	TCg TTg gAT CAC AgC ACA TCA	TCg TTg gAT CAC AgC ACA TCA
VEGF	CTT gCC TTg CTg CTC TAC CTC C	CAT CCA TgA ACT TCA CCA CTT CgT

Real-time polymerase chain reaction

Total RNA from cell lines was extracted using NucleoSpinRNAII (Macherey Nagel). Total RNA from tumors was extracted using the TRizol reagent (Invitrogen Life Technologies) after mechanical grinding with Turrax (IKA). qRT-PCR were performed as previously described (27). Primer sequences are provided in Table 1.

Transient cell transfections, reporter assays, and plasmid constructs

Transient cell transfections were performed with jetPEI (polyplus-transfection). The phRLMLP-*Renilla* luciferase expression vector was cotransfected in all experiments to monitor transfection efficiencies. Luciferase activity was determined with the dual-luciferase reporter assay system (Promega). The $(CAGA)_9$-Luc construct was used as a reporter construct specific for Smad3/4-driven signaling (28). The pcDNA-Smad7 vector is a kind gift from Dr. Alain Mauviel (19).

Osteosarcoma mouse model

Four-week-old female Rj:NMRI-nude mice (Elevages Janvier) were maintained under pathogen-free conditions at the Experimental Therapy Unit (Faculty of Medicine, Nantes, France) in accordance with the institutional guidelines of the French Ethical Committee (CEEA Pays de la Loire No. 06; project authorization No. CEEA-2010-23) and under the supervision of authorized investigators. The mice were anesthetized by inhalation of an isoflurane/air mixture (1.5%, 1 L/min) before receiving an intramuscular injection of 1×10^6 HOS or SaOS2 osteosarcoma cells in close proximity to the tibia, leading to a rapidly growing tumor in soft tissue with secondary contiguous bone invasion. One day after HOS cells injection, some mice received different doses (20 or 60 mg/kg) of SD-208 or control vehicle by daily gavage. The tumor volume (V) was calculated from the measurement of 2 perpendicular diameters using a caliper, according to the following formula: $V = 0.5 \times L \times (S)^2$, as previously described (29). Mice were sacrificed when the tumor volume reached 2,500 mm^3 for ethical reasons. Under these conditions, pulmonary metastasis developed when tumor volumes were $\geq$2,000 mm^3.

Micro-CT analysis

Analysis of bone microarchitecture was performed as previously described (27) at different tumor volumes (250, 1,000, and 2,500 mm^3). All tibiae/fibulae were scanned using the same parameters (pixel size 18 μm, 50 kV, 0.5-mm Al filter, and 0.8 degrees per rotation step). Three-dimensional reconstructions and analysis of bone parameters were performed using the CTvol and CTan software (Skyscan).

Histologic analysis

After sacrifice, the tibiae were conserved and fixed in 10% buffered formaldehyde, decalcified (4% EDTA, 0.2% paraformaldehyde, pH 7.4), and embedded in paraffin. Three-micrometer sections of tumor-bearing tibiae were cut and stained for tartrate-resistant acid phosphatase (TRAP) to analyze osteoclast activity. Lungs were fixed in 10% buffered formaldehyde and embedded in paraffin. Lung sections (3-μm-thick) were mounted on glass slides and stained with hematoxylin–eosin (HE).

Immunohistochemistry of human and mice tumor samples

Three-micrometer sections of human tumor tissues (embedded in paraffin) were cut and stained for phospho-Smad3 using rabbit polyclonal anti–phospho-Smad3 antibody (Abcam). Patient tumor clinical samples collected at Nantes University Hospital (Nantes, France) were obtained following patient informed consent and after ethical approval by the Nantes University Hospital Ethics Committee.

Sections (3 μm) of mice tumor tissues (embedded in paraffin) were cut and stained for osterix, RANKL, osteocalcin, caspase-3, Ki67, and CD146 using, respectively, rabbit polyclonal anti-osterix (Abcam), anti-RANKL (Santa Cruz Biotechnology), anti-osteocalcin (Abcam), anti–caspase-3 (Cell Signaling), anti-Ki67 (Dako), anti CD146 (Abcam) antibodies. Immunodetection was performed

Published OnlineFirst August 8, 2014; DOI: 10.1158/1078-0432.CCR-13-3191

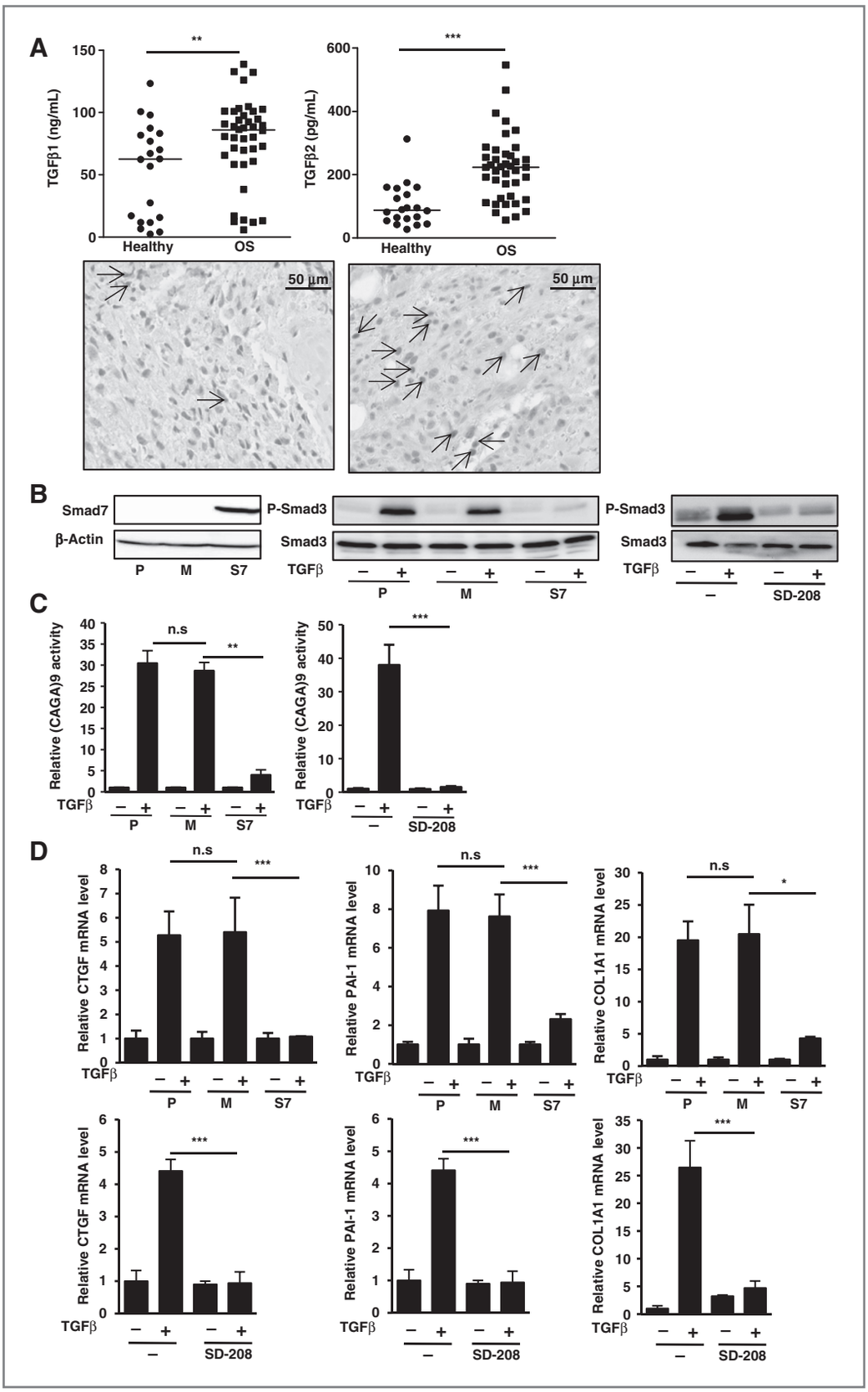

Published OnlineFirst August 8, 2014; DOI: 10.1158/1078-0432.CCR-13-3191

using DAB Substrate-Chromogen (Dako) and counterstained with hematoxylin.

Collagen degradation

The degradation of collagen was evaluated by the measure of pyridinoline excretion in mice serum using the MicroVue Serum PYD EIA Kit.

Transwell motility and invasion

Osteosarcoma cells (30,000 cells/well) were pretreated with 5 ng/mL TGFβ in the presence or absence of SD-208 (10μmol/L) for 24 hours and seeded onto the upper surface of transwell inserts (Falcon) coated with 0.1 mg/mL of growth factor–reduced Matrigel (Biocoat; BD Biosciences) for the invasion assay, or on uncoated transwells (migration assay) and incubated at 37°C for 48 hours. At the end of the incubation period, cells on the upper surface of the inserts were wiped off, and the cells on the underside of the membrane were fixed, stained with "cristal violet" and counted by bright-field microscopy in 5 random fields.

Gelatin zymography

Cells were cultured for 48 hours without serum and their conditioned media were analyzed by gelatin zymography in 10% polyacrylamide gels containing 1 mg/mL gelatin (Sigma-Aldrich) as described previously (19).

Statistical analysis

All analyses were performed using GraphPad Prism 4.0 software (GraphPad Software). Results of *in vitro* experiments were analyzed with the unpaired *t*-test and are given as means ± SD. For *in vivo* experiments, results from groups overexpressing Smad7 were compared with control groups (parental and mock) and results from mice treated with SD-208 were compared with untreated mice using the unpaired *t*-test and are given as means ± SEM. Results of animal survival were analyzed using the log-rank test. Results with $P < 0.05$ were considered significant.

Results

High levels of TGFβ1 and TGFβ2 are measured in serum samples from patients with osteosarcoma

TGFβ1, TGFβ2, and TGFβ3 levels were measured in the serum samples of 40 patients with osteosarcoma and compared with 20 age-matched healthy volunteers. As shown in Fig. 1A (top), TGFβ1 (left) and TGFβ2 (right) concentrations measured in the serum were significantly higher in the serum samples of patients with osteosarcoma compared with healthy volunteers ($P < 0.01$ and $P < 0.0001$ for TGFβ1 and TGFβ2, respectively). Note that the TGFβ3 serum levels were very low, under the limit of detection in our experimental conditions (not shown). Second, immunohistochemical experiments were performed to analyze the levels of phospho-Smad3 in 6 clinical samples of patients with osteosarcoma. As shown in Fig. 1A (bottom), a high level of phospho-Smad3 was detected in the nucleus of osteosarcoma cells, demonstrating the activation of the TGFβ/Smad3 cascade. Interestingly, this level of phospho-Smad3 was higher in clinical samples from patients with pulmonary metastasis than without pulmonary metastasis at diagnosis (Fig. 1A, right vs. left).

Overexpression of Smad7 and a chemical inhibitor of TβRI (SD-208) block the TGFβ/Smad3 signaling pathway in osteosarcoma cells

To evaluate the effect of Smad7 overexpression on osteosarcoma growth and progression, 2 human osteosarcoma cell lines (HOS and SaOS2) were stably transfected with either empty pcDNA or pcDNA-Smad7 encoding *Smad7*. First, endogenous Smad7 was not detectable in either parental or mock-transfected HOS and SaOS2 cells, whereas Smad7-transfected osteosarcoma cells expressed high levels of the protein (Fig. 1B, left and Supplementary Fig. S1A). Second, Smad7 expression inhibits the ability of TGFβ to induce the phosphorylation of Smad3 (Fig. 1B, middle), to transactivate the Smad3/4-specific reporter construct $(CAGA)_9$-luc (Fig. 1C, left), and to stimulate the expression of *CTGF*, *PAI-1*, and *COL1A1* (Fig. 1D, top). Similar results were obtained with the SaOS2 cell line (Supplementary Fig. S1). Note that the overexpression of Smad7 partially inhibits a BMP-specific target gene such as *ID1* (Supplementary Fig. S1C) but not the ability of TGFβ to induce the activation of MAPKinases such as $ERK_{1/2}$ (Supplementary Fig. S1D). To specifically target the TGFβ cascade, we secondly studied the effect of a TβRI inhibitor, the chemical compound SD-208. As expected, SD-208 (10 μmol/L) effectively blocks the ability of TGFβ to induce

Figure 1. Evaluation of TGFβ levels in serum of patients with osteosarcoma. Overexpression of Smad7 and SD-208 in HOS cells block the TGFβ/Smad3 cascade. A, top, comparison of TGFβ1 (left) and TGFβ2 (right) levels in serum from healthy age-matched controls ($n = 20$) or patients with osteosarcoma ($n = 40$; median; ***, $P < 0.005$; **, $P < 0.01$); bottom, clinical tumor samples of patients with osteosarcoma with ($n = 3$, right) or without ($n = 3$, left) pulmonary metastasis at diagnosis were immunostained with phospho-Smad3 antibody. One representative photomicrograph per group is shown. Arrows indicate the localization of P-Smad3 in the nucleus of osteosarcoma cells. B, left: Smad7 production was detected by Western blot analysis in HOS cells [parental (P), mock- (M), and Smad7-transfected cells (S7)]; middle: phospho-Smad3 and Smad3 were detected by Western blot analysis in parental (P), mock- (M), and Smad7-transfected (S7) HOS cells treated or not with TGFβ1 (5 ng/mL) for 15 minutes; right: parental HOS cells were treated with TGFβ (5 ng/mL, 15 minutes) in the presence or absence of SD-208 (10 μmol/L). After incubation, phospho-Smad3 and Smad3 levels were detected by Western Blot analysis of whole cell lysates. C, cells were transfected with the Smad3/4-specific construct $(CAGA)_9$-luc. Twenty-four hours after transfection, TGFβ (5 ng/mL) was added and incubation was continued for another 48 hours in the presence or absence of SD-208 (10 μmol/L) as indicated. Bars, means ± SD of at least three independent experiments, each performed in duplicate (***, $P < 0.005$; **, $P < 0.01$). D, cells were treated with TGFβ1 (5 ng/mL) for 6 or 24 hours in the presence or absence of SD-208 (10 μmol/L as indicated). After incubation, mRNA steady-state levels of the specific TGFβ target genes *CTGF* (6 hours), *PAI-1* (24 hours), and *COL1A1* (24 hours) were determined by quantitative RT-PCR. Bars, means ± SD of at least three independent experiments, each performed in duplicate (***, $P < 0.005$; *, $P < 0.05$).

Published OnlineFirst August 8, 2014; DOI: 10.1158/1078-0432.CCR-13-3191

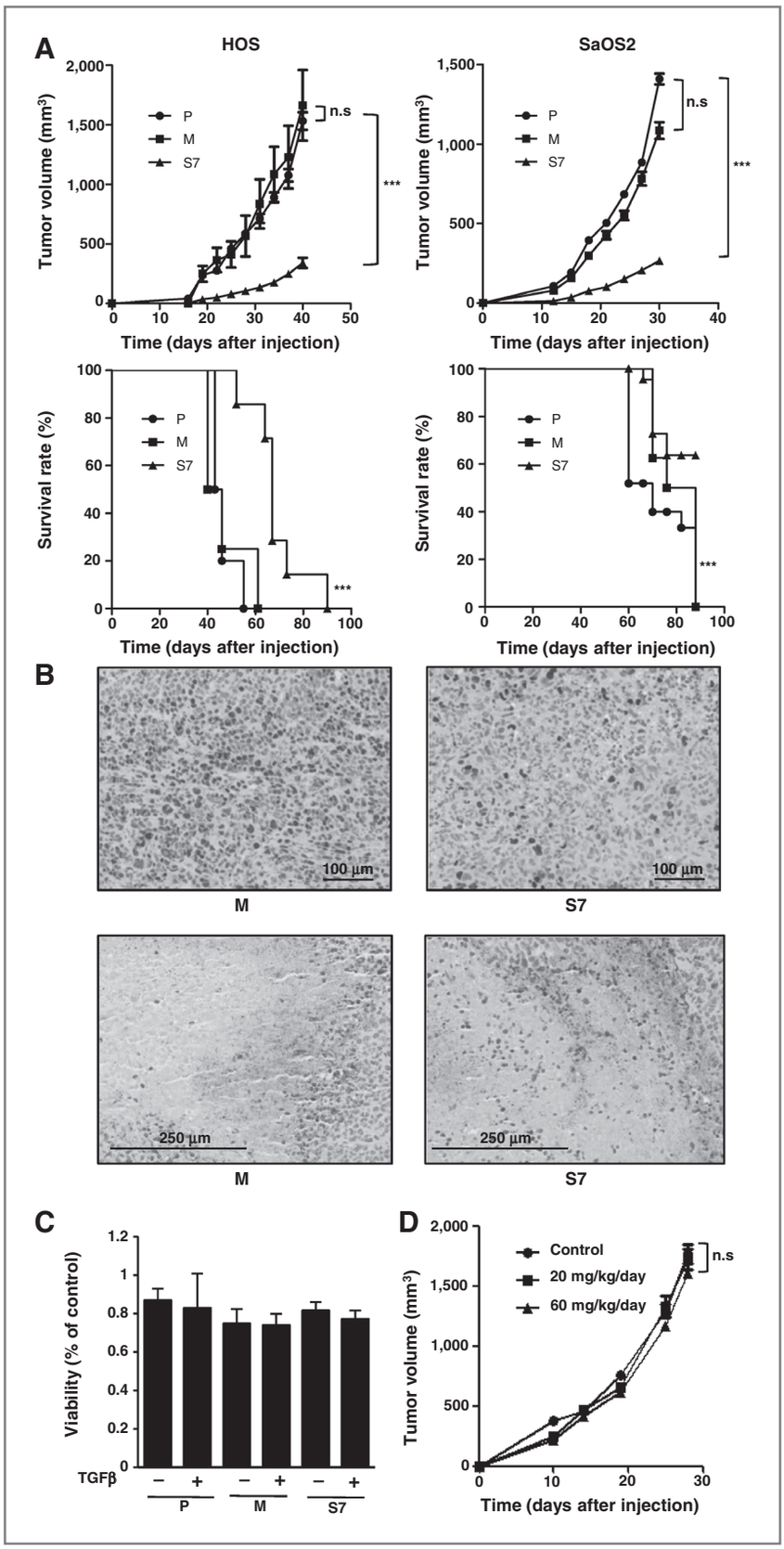

Figure 2. Overexpression of Smad7 inhibits tumor growth in the HOS and SaOS2 osteosarcoma models and improves animal survival. A, mice were injected either with 1×10^6 parental (P), mock- (M), and Smad7-transfected (S7) HOS cells ($n = 10$ for parental, $n = 4$ for mock, and $n = 7$ for Smad7 cells, left) or with 1×10^6 parental (P), mock- (M), and Smad7-transfected (S7) SaOS2 cells ($n = 22$ for parental, $n = 8$ for mock, and $n = 22$ for Smad7 cells, right). The results are representative of 2 independent experiments (mean ± SEM; ***, $P < 0.005$). Top, the mean tumor volumes were calculated from day 1 to day 40 for HOS group (left) or from day 1 to day 30 for SaOS2 group (right). Bottom, overall survival rates for each groups. The survival rates were calculated from day 1 to day 90, when the last mouse was euthanized (in the Smad7 group). B, tumor samples (tumor sizes at 250 mm^3) of the mock and Smad7 HOS group were fixed, embedded in paraffin, sectioned, and stained with KI67 (top) or caspase-3 (bottom). Representative photomicrographs per group for HOS osteosarcoma mice are shown. C, parental (P), mock- (M), and Smad7-transfected (S7) HOS cells were treated with TGFβ1 (5 ng/mL) for 6 days. After incubation, cell viability was evaluated by XTT test. Bars, means ± SD of two independent experiments, each performed in 6 replicate. D, intramuscular paratibial injections of 1×10^6 HOS tumor cells were performed in 3 groups of nude mice (vehicle, SD-208 20 mg/kg/day and SD-208 60 mg/kg/day, $n = 6$ mice for each group). The mean tumor volumes were calculated from day 1 to day 28.

Published OnlineFirst August 8, 2014; DOI: 10.1158/1078-0432.CCR-13-3191

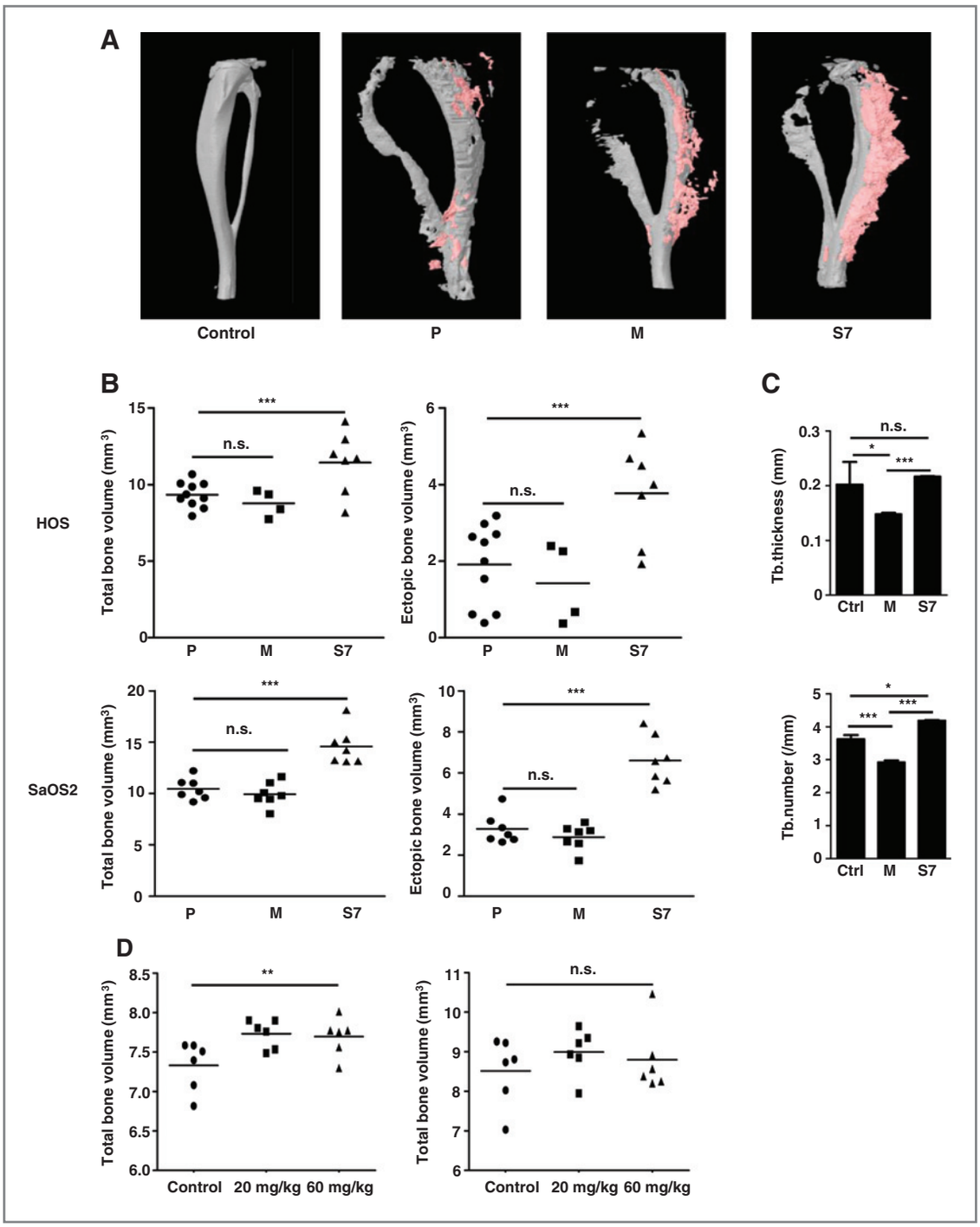

Figure 3. Overexpression of Smad7 in tumor cells inhibits tumor-associated bone resorption. Mice were either injected with 1×10^6 parental (P), mock- (M), and Smad7-transfected (S7) HOS cells ($n = 10$ for parental, $n = 4$ for mock and $n = 7$ for Smad7 cells) or with 1×10^6 parental (P), mock- (M), and Smad7-transfected (S7) SaOS2 cells ($n = 7$ for parental, $n = 7$ for mock, and $n = 7$ for Smad7). The results are representative of 2 independent experiments. A, 3D reconstructions of one representative tibia/fibula of each group (parental, mock, and Smad7 HOS cells) were performed when tumor sizes were approximately 2,500 mm^3 and compared with a healthy group bearing no tumors (control). B, left: graphs represent the total bone volume of each individual animal in a given group injected with either HOS cells (top) or with SaOS2 cells (bottom; ***, $P < 0.005$); right: graph represents the mean ectopic bone volume of each individual animal in a given group injected with either HOS cells (top) or with SaOS2 cells (bottom; ***, $P < 0.005$). C, histograms represent the mean trabecular (Tb.) thickness (top) and the number of bone trabecular (bottom) in mock and Smad7 HOS groups compared with control group corresponding to mice bearing no tumors (***, $P < 0.005$; *, $P < 0.05$). D, intramuscular paratibial injections of 1×10^6 HOS tumor cells were performed in 3 groups of nude mice (vehicle, SD-208 20 mg/kg/day and SD-208 60 mg/kg/day). The bone volumes of tibia were measured both at the leg having undergone the injection of tumor cells (right) and at the counterpart legs (left) when tumor volume reached 1,000 mm^3. Graphs represent the bone volume of each individual animal in a given group (**, $P < 0.01$).

Published OnlineFirst August 8, 2014; DOI: 10.1158/1078-0432.CCR-13-3191

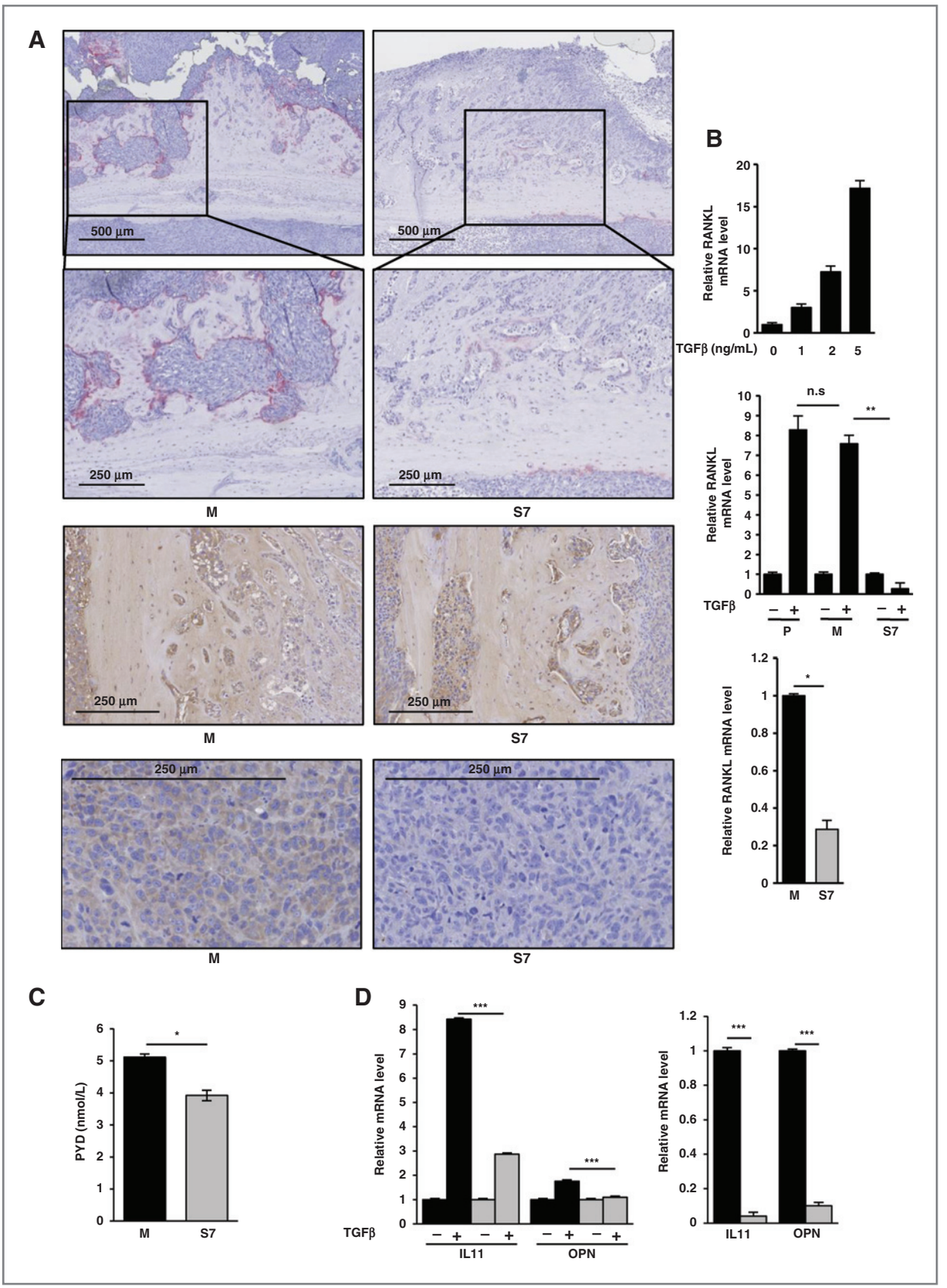

Published OnlineFirst August 8, 2014; DOI: 10.1158/1078-0432.CCR-13-3191

the phosphorylation of Smad3 (Fig. 1B, right), to transactivate the Smad3/4-specific reporter construct $(CAGA)_9$-luc (Fig. 1C, right), and to stimulate the expression of *CTGF*, *PAI-1*, and *COL1A1* (Fig. 1D, bottom) in HOS cells and in SaOS2 cells (Supplementary Fig. S1). Note that in contrast to Smad7 overexpression, the SD-208 inhibitor is able to block the ability of TGFβ to activate the phosphorylation of $ERK_{1/2}$ (Supplementary Fig. S1D, bottom).

These results confirmed that both Smad7 overexpression and SD-208 block the TGFβ/Smad3 cascade in osteosarcoma cells.

Overexpression of Smad7 in osteosarcoma cell lines dramatically inhibits *in vivo* tumor growth

A preclinical experimental model of osteosarcoma induced by paratibial injection of osteosarcoma cells was developed. Smad7 overexpression in HOS or SaOS2 cells inhibited tumor growth in both models (Fig. 2A, top). The mean tumor size at day 40 in mice injected with parental or mock-transfected HOS cells was 1,531.8 ± 73.4 mm^3 and 1,663.9 ± 297.0 mm^3 respectively, compared with only 341.5 ± 43.4 mm^3 in mice injected with HOS-S7 cells (means ± SEM, $P < 0.005$; Fig. 2A, top HOS panel). Similar results were obtained in the SaOS2 model (Fig 2A, top SaOS2 panel). Consequently, Smad7 overexpression resulted in an increased animal survival in both models (Fig. 2A, bottom). In this context, immunohistochemical staining for the proliferative marker Ki67 in tumor samples from mice showed that Smad7 overexpression decreased cell proliferation as compared with the mock-transfected group (Fig. 2B, top) when the tumor sizes reached 250 mm^3. By contrast, caspase-3 immunostaining of the same samples showed no significant difference between mice injected with Smad7-transfected cells and animals receiving mock-transfected cells (Fig. 2B, bottom). To better understand the mechanisms underlying the effect of Smad7 on osteosarcoma tumor growth, we next carried out *in vitro* experiments. Interestingly, treatment of osteosarcoma cells with TGFβ (5 ng/mL) did not affect osteosarcoma cell proliferation even after 6 days of TGFβ treatment, whether the cells expressed Smad7 or not (Fig. 2C). In contrast to the effect of Smad7 overexpression, the treatment of mice with SD-208 (20 or 60 mg/kg/day) does not affect the *in vivo* tumor growth of osteosarcoma (Fig. 2D).

These results demonstrate that overexpression of Smad7 reduced *in vivo* tumor growth and suggest that this effect is not because of a direct effect of Smad7 on osteosarcoma cell proliferation.

Smad7 overexpression in HOS and SaOS2 osteosarcoma cells inhibits tumor-associated bone resorption

Because osteosarcoma-associated alteration of bone remodeling plays a central role in the development and progression of osteosarcoma bone tumors, we evaluated the ability of Smad7 and SD-208 to alter tumor-associated bone remodeling. The microarchitecture of bone in mice bearing osteosarcoma tumors was first examined when the tumor sizes reached 2,500 mm^3 using a high-resolution X-ray micro-CT system.

Visual inspection of the 3D reconstructions of the tibia suggests that Smad7 overexpression enhanced the tumor-associated bone formation in HOS osteosarcoma models (Fig. 3A). Indeed, the total bone volume in mice injected with parental or mock-transfected HOS cells was 9.34 ± 0.08 and 8.77 ± 0.15 mm^3 respectively, compared with 11.44 ± 0.28 mm^3 in mice bearing HOS-S7 tumors ($P < 0.005$; Fig. 3B, HOS left panel). Similarly, Smad7 overexpression enhanced total bone volume in mice injected with SaOS2 cells (Fig. 3B, SaOS2 left panel).

We next determined whether this increase in total bone volume was due either to direct new bone formation (ectopic bone) and/or to an inhibition of bone resorption. As shown in Fig. 3B (HOS right panel), the ectopic bone volume in mice injected with parental or mock-transfected HOS cells was significantly lower than in mice bearing HOS-S7 tumors (1.91 ± 0.11 mm^3 and 1.43 ± 0.26 mm^3 vs. 3.77 ± 0.18 mm^3 respectively, $P < 0.005$). Similarly, Smad7 enhanced ectopic bone volume in the SaOS2 model ($P < 0.005$; Fig. 3B, SaOS2 right panel). We then analyzed the ability of Smad7 to alter bone osteolysis by evaluating the trabecular number (Tb.N) and trabecular thickness (Tb.Th) when tumor sizes were around 250 mm^3, because at higher volumes (1,000 mm^3 or 2,500 mm^3) trabecular bone is completely destroyed by the tumor cells (data not shown). As shown in Fig. 3C (top), mice injected

Figure 4. Overexpression of Smad7 in osteosarcoma reduces osteoclast activity. A, tumor samples (tumor sizes at 1,000 mm^3) of the mock and Smad7 group were fixed, embedded in paraffin, sectioned, and stained for TRAP (red stained cells, top), osteocalcin (middle), and RANKL (bottom). Representative photomicrographs per group for HOS osteosarcoma mice are shown. B, *RANKL* mRNA steady-state levels were determined by quantitative RT-PCR in the presence or absence of TGFβ as indicated. Bars, mean ± SD of at least three independent experiments carried out in duplicate (top). Parental (P), mock- (M), and Smad7-transfected (S7) HOS cells were treated with TGFβ1 (5 ng/mL) for 24 hours. After incubation, *RANKL* mRNA steady-state levels were determined by quantitative RT-PCR (middle). RNA was extracted from tumor biopsies of mice injected with mock- (black) or Smad7 (gray) transfected HOS cells. *RANKL* mRNA steady-state levels were determined by quantitative RT-PCR (bottom). Bars, means ± SD of at least 3 independent experiments, performed in duplicate (*, $P < 0.05$; **, $P < 0.01$). C, concentrations of pyridinoline in mice serum of the mock and Smad7 groups were measured using the MicroVue Serum PYD EIA Kit. Bars, means ± SEM of two independent experiments, performed in duplicate (*, $P < 0.05$). D, left: treatment of mock- (black) and Smad7-transfected (gray) HOS cells with TGFβ1 (5 ng/mL) for 24 hours. After incubation, *IL11* and *OPN* mRNA steady-state levels were determined by quantitative RT-PCR. Bars, mean ± SD of at least 3 independent experiments carried out in duplicate (***, $P < 0.005$); right: RNA was extracted from tumor biopsies of mice injected with mock- (black) and Smad7 (gray) transfected HOS cells. *IL11* and *OPN* mRNA steady-state levels were determined by quantitative RT-PCR. Bars, mean ± SD of 2 independent experiments carried out in duplicate (***, $P < 0.005$).

Published OnlineFirst August 8, 2014; DOI: 10.1158/1078-0432.CCR-13-3191

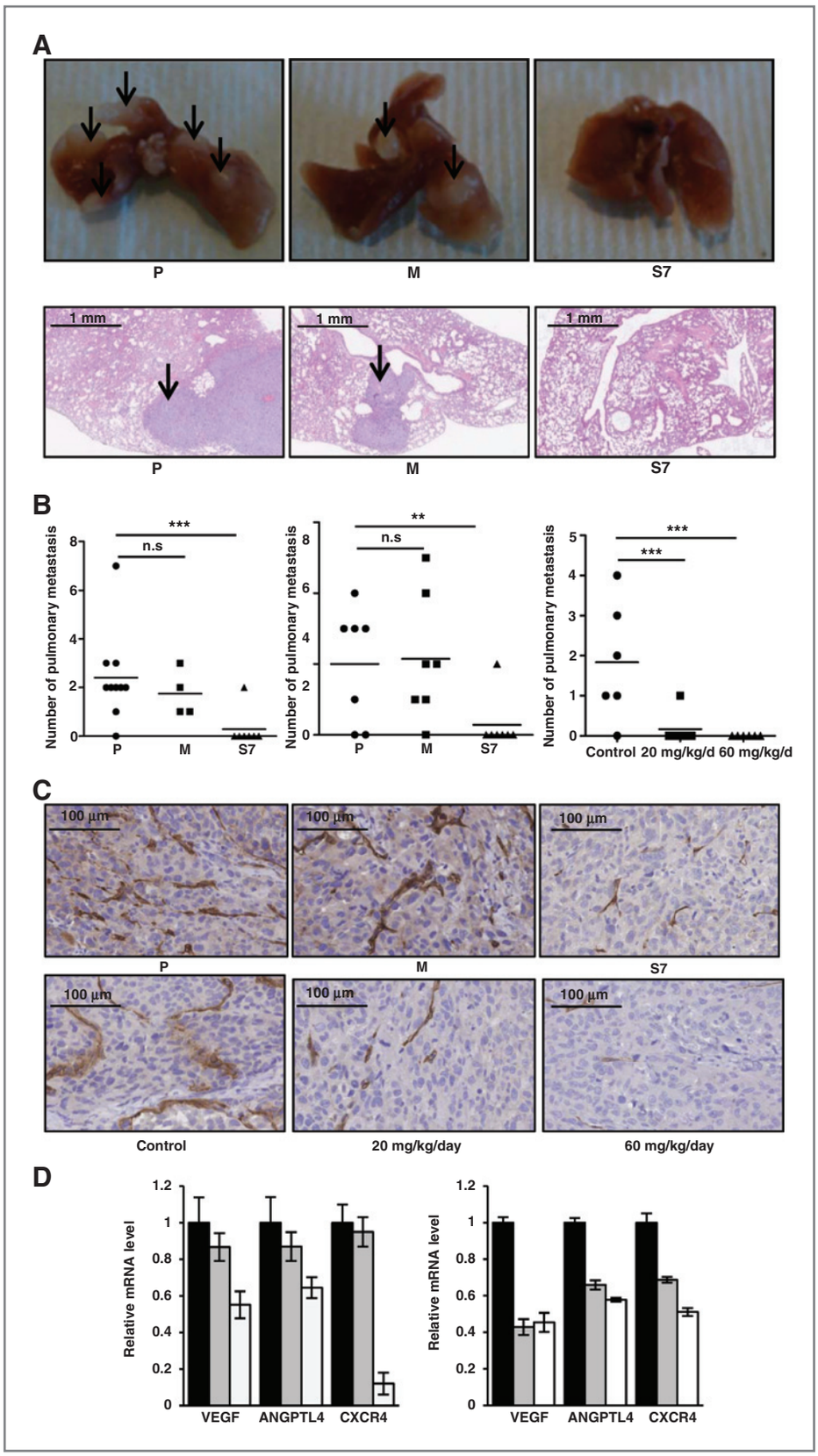

Figure 5. Overexpression of Smad7 in osteosarcoma and treatment of mice with SD-208 block lung metastasis development. Mice were either injected with parental (P), mock- (M), and Smad7-transfected (S7) osteosarcoma cells (HOS or SaOS2) or injected with parental-HOS cells and treated with vehicle or SD-208 as indicated. Mice were sacrificed when tumor sizes reached 2,500 mm^3 and lungs were removed. A, photographs of representative lungs of P, M, and S7 HOS group. Arrows point to lung metastasis (top). H&E staining of lungs. Arrows indicate metastatic tumor cells (bottom). B, graphs indicate individual (dots) and mean (lines) numbers of lung metastasis measured in lungs from each group (***, $P < 0.005$; **, $P < 0.01$), respectively for P, M, and S7-HOS model (left), P, M, and S7-SAOS2 model (middle) and for mice treated or not with SD-208 (right). C, tumor samples (tumor sizes at 2,500 mm^3) of the P, M, and S7 group (top) and from mice treated or not with SD-208 as indicated (bottom) were fixed, embedded in paraffin, sectioned, and stained with CD146. Representative photomicrographs per group for HOS osteosarcoma mice are shown. D, RNA was extracted from tumor biopsies of mice injected with P (black), M (gray), and S7 (white) transfected HOS cells (left) or from tumor biopsies from mice treated with SD-208 at 20 mg/kg/day (gray), SD-208 at 60 mg/kg/day (white), or with vehicle (black; right). *VEGF, ANGPTL4*, and *CXCR4* mRNA steady-state levels were determined by quantitative RT-PCR. Bars, mean ± SD of 2 independent experiments carried out in duplicate.

Published OnlineFirst August 8, 2014; DOI: 10.1158/1078-0432.CCR-13-3191

with mock-transfected HOS cells had a lower Tb.Th than mice bearing HOS-S7 tumors (0.15 ± 0.01 mm vs. 0.22 ± 0.01 mm, $P < 0.005$). Moreover, the Tb.N was also lower in the mock group than in the HOS-S7 tumor-bearing group (2.92 ± 0.03 mm vs. 4.18 ± 0.02 mm; $P < 0.005$; Fig. 3C, bottom). Note that Tb.Th and Tb.N in mice bearing HOS-S7 tumors are similar to those observed in healthy control mice. Interestingly, although the treatment of mice with SD-208 affects bone remodeling with a significant increase of tibia bone volume in the absence of tumor (Fig. 3D, left) as previously described (30), the SD-208 does not affect significantly the tumor-associated bone remodeling (Fig. 3D, right).

These results demonstrate that in contrast with SD-208 mice treatment, overexpression of Smad7 in osteosarcoma cells both decreased tumor-associated bone osteolysis and promoted tumor-associated bone formation.

Overexpression of Smad7 in HOS and SaOS2 osteosarcoma cells reduces osteoclast activity

The activity of osteoclasts and osteoblasts, 2 cell lineages implicated in bone remodeling, was then assessed during the early stages of tumor growth (tumor size $\leq$250 mm^3 or $\leq$1,000 mm^3). TRAP staining in sections of tumor-bearing tibia showed that HOS-S7 tumor cells reduced the number of $TRAP^+$ multinucleated cells at the interface between tumor and cortical bone (Fig. 4A, top) and in the growth plate (not shown), relative to the control conditions at the same tumor size (1,000 mm^3). Similar results were obtained when tumors had reached 250 mm^3 (data not shown). By contrast, osteocalcin (Fig. 4A, middle) and osterix (data not shown) immunostaining of the same samples showed no significant difference between mice injected with Smad7-transfected cells and animals receiving mock-transfected cells.

To understand the effect of Smad7 on osteoclast activity, we analyzed *RANKL* gene expression in HOS osteosarcoma cell lines. qRT-PCR analysis indicated that the mRNA steady-state level of *RANKL* was increased in response to TGFβ and that Smad7 overexpression prevented such induction (Fig 4B, top and middle, respectively). Moreover, Smad7 overexpression decreased RANKL production by HOS tumor cells (Fig. 4A, bottom) evaluated by immunohistochemical experiments. In accordance with this observation, HOS-S7 bone tumors expressed significantly lower mRNA levels of *RANKL* (Fig. 4B, bottom). Finally, the degradation of collagen evaluated by the measure of pyridinoline excretion in mice serum is decreased when Smad7 is overexpressed in osteosarcoma cells (Fig. 4C).

In addition to *RANKL*, the expression of other TGFβ target genes implicated in bone remodeling (18, 20, 21) such as *interleukin-11* (IL11) and *osteopontin* (OPN) is decreased when Smad7 is overexpressed. As shown in Fig. 4D, q-PCR analysis indicated that the *IL11* and *OPN* expressions were increased in response to TGFβ and that Smad7 overexpression prevented such induction (Fig 4D, left). HOS-S7 bone tumors expressed significantly lower levels of *IL11* and *OPN* mRNA (Fig. 4D, right).

These results demonstrate that Smad7 overexpression decreases osteoclast activity and thus bone osteolysis at least in part via the modulation of osteolytic genes such as *RANKL*.

Overexpression of Smad7 in HOS and SaOS2 osteosarcoma cells or treatment of mice with SD-208 inhibits dissemination of pulmonary metastasis

To evaluate the effect of Smad7 on pulmonary metastasis development (Fig. 5A), the lungs of mice were removed when primary tumor volumes reached 2,500 mm^3. As shown in Fig. 5B, a high incidence of pulmonary metastasis was observed in mice inoculated with parental or mock-transfected HOS cells, respectively 9 of 10 (90%) and 4 of 4 (100%) mice. By contrast, only 1 of 7 (14%) mice bearing HOS-S7 cells developed lung metastasis (Fig. 5B, left). As shown in Fig. 5B (middle), similar results were obtained in the SaOS2 model. Remarkably, the treatment of mice with SD-208 inhibits the development of lung metastasis. As shown in Fig. 5B (right), 5 of 6 (83.3%) mice treated with vehicle (control group) developed lung metastasis. By contrast, only 1 of 6 (16.7%) mice treated with 20 mg/kg/day developed lung metastasis, and no mice treated with 60 mg/kg/day developed lung metastasis. Interestingly, immunohistochemical staining for the endothelial marker CD146 in mice tumor samples showed that Smad7 overexpression or SD-208 treatment dramatically decreased the angiogenic process as compared respectively with the parental and mock-transfected groups or with the untreated group (Fig. 5C). In addition, qPCR analysis from mice biopsies indicated that the expression by tumor cells of *VEGF* (implicated in the angiogenic process), and *CXCR4* and *ANGPTL4* (respectively identified as key players to prime breast cancer cells for metastasis toward the lungs and/or the bones) were both reduced when Smad7 was overexpressed or when mice were treated with SD-208 (Fig. 5D).

The influence of Smad7 overexpression in osteosarcoma cells or the treatment of tumor cells with SD-208 was then examined on several aspects of tumor cell behavior *in vitro*. As shown in Fig. 6 and in Supplementary Fig. S2, Smad7 overexpression in HOS and SaOS2 cells or treatment of HOS cells with SD-208 lead to a strongly reduced capacity of TGFβ to stimulate cell migration (Fig. 6A and Supplementary Fig. S2A) and invasion (Fig. 6B and Supplementary Fig. S2B). In addition, exogenous TGFβ-induced secretion of the active form of matrix metalloproteinase MMP2 was strongly diminished both in Smad7-transfected cells and in cells treated with SD-208 (Fig. 6C and supplementary Fig. S2C). qRT-PCR analysis indicated a reduction of TGFβ-induced *MMP2* mRNA levels in Smad7-transfected– or SD-208–treated cells (Fig. 6D, top). *MMP2* mRNA steady-state levels were increased by approximately 5-fold in parental and mock-transfected HOS cells, but only by 2-fold in HOS-S7 cells after

Published OnlineFirst August 8, 2014; DOI: 10.1158/1078-0432.CCR-13-3191

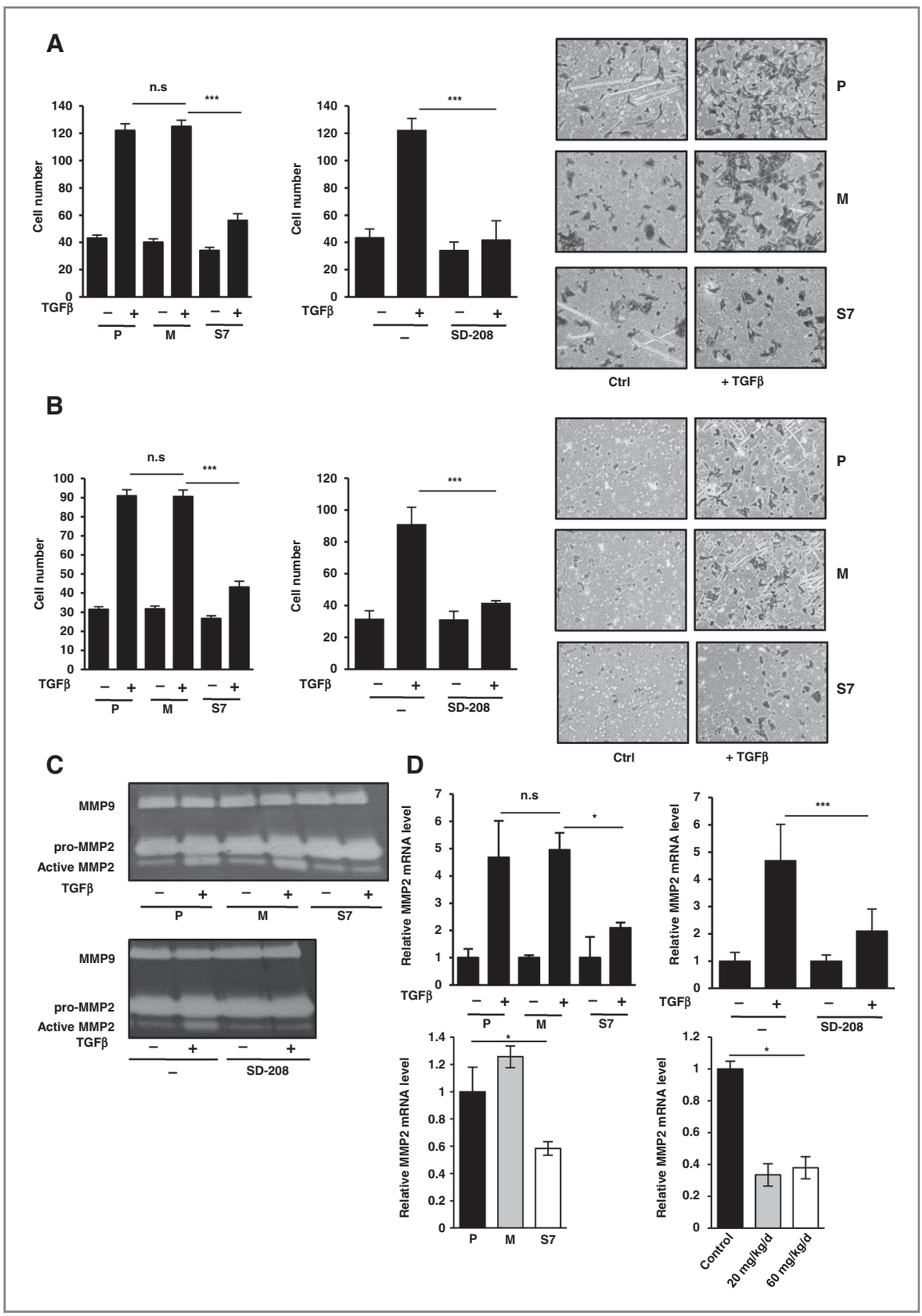

Published OnlineFirst August 8, 2014; DOI: 10.1158/1078-0432.CCR-13-3191

treatment of osteosarcoma cells with TGFβ (5 ng/mL) for 24 hours. Similar results were obtained when Smad7 was overexpressed in SaOS2 cells (Supplementary Fig. S2D) or when osteosarcoma cells were treated with SD-208 (Fig. 6D, right and Supplementary Fig. S2D, right). In addition, both HOS-S7 bone tumors and HOS cells from mice treated with SD-208 expressed significantly lower levels of *MMP2* (Fig. 6D, bottom).

These results demonstrated that overexpression of Smad7 in osteosarcoma cells or treatment of mice with SD-208 blocks the formation of lung metastasis.

Discussion

Increased TGFβ1 mRNA and/or protein expression has been correlated with a wide range of cancers such as colorectal cancer, gastric carcinoma, or prostate cancer (31–34). This increase in serum TGFβ1 production and/or TGFβ1 staining in tumor cells has been associated with disease progression to metastasis in these carcinomas (31). Here, we demonstrated that high concentrations of TGFβ1 and TGFβ2 measured in serum of patients is associated with osteosarcoma disease. In addition, using clinical samples, we demonstrated that the Smad3 cascade is activated in osteosarcoma cells particularly in high-risk patients when lung metastasis are detected at diagnosis. Previous studies have reported that high levels of *TGFβ1* mRNA in tumor cells are associated with high-grade osteosarcoma, which shows an aggressive behavior and frequently metastasizes to lung or other sites (24). These observations together with our results suggest that high levels of TGFβ1 in serum could be associated with a poor prognosis in osteosarcoma.

Following these observations, we first inhibited the Smad signaling cascade in osteosarcoma cells via the overexpression of the inhibitory Smad, Smad7, and then we used the chemical inhibitor of TβRI, SD-208, to specifically inhibit the signaling cascade downstream the receptor TβRI. By using various *in vitro* approaches, we demonstrated that Smad7 overexpression and SD-208 efficiently inhibit the TGFβ transcriptional response mediated by Smad3/4 in 2 human osteosarcoma cell lines, HOS and SaOS2.

Using a murine model of osteosarcoma induced by paratibial injection of osteosarcoma cells overexpressing Smad7, we then demonstrated that Smad7 overexpression slows primary tumor growth, a process associated with a reduction of the immunohistochemical staining for the proliferative marker Ki67. Because TGFβ is a cytokine widely implicated in the control of cell proliferation (17), the effect of TGFβ and overexpression of Smad7 was studied on osteosarcoma cell proliferation *in vitro*. In contrast to previous observations that demonstrated an effect of TGFβ on cell proliferation (35, 36), no effect of TGFβ and/or Smad7 overexpression was observed on the *in vitro* proliferation rate of osteosarcoma cells under our experimental conditions, suggesting that Smad7 does not directly affect the proliferation of osteosarcoma cells but rather affects the tumor microenvironment indirectly involved in the control of tumor cell proliferation.

In this context, because osteosarcoma-associated alterations of bone remodeling play a central role in the development and progression of osteosarcoma, we studied the effect of Smad7 on bone remodeling. We clearly demonstrated that Smad7 overexpression in osteosarcoma cells slows bone destruction associated with the tumor growth. In this context, we demonstrated that this process was mainly associated with a reduction of trabecular bone destruction during the early stages of tumor growth (when tumor volumes were below 250 mm^3) and with an increase of ectopic bone formation during the late stages of tumor growth (when tumor volumes were greater than 1000 mm^3). The presence of a "vicious cycle" established between tumor proliferation and paratumor osteolysis plays a crucial role in the

Figure 6. Overexpression of Smad7 in osteosarcoma cells or treatment of cells with SD-208 inhibit the ability of TGFβ to induce osteosarcoma cell migration and invasion. A and B, left: 30,000 parental, mock-, or Smad7-transfected HOS cells pretreated during 24 hours with 5 ng/mL TGFβ were seeded onto the upper surface of uncoated (A) or transwell coated with 2 μg Matrigel (B) inserts. Forty-eight hours after incubation in the presence or absence of TGFβ (5 ng/mL), the cells on the underside of the membrane were fixed, stained with "cristal violet," and counted by bright-field microscopy in 5 random fields (magnification: ×200). Bars, mean ± SD of at least 3 independent experiments carried out in duplicate (***, $P < 0.005$); middle: 30,000 parental HOS cells pretreated during 24 hours with 5 ng/mL TGFβ in the presence or absence of SD-208 (as indicated) were seeded onto the upper surface of uncoated (A) or transwell coated with 2 μg Matrigel (B) inserts. Forty-eight hours after incubation in the presence or absence of TGFβ (5 ng/mL) and SD-208 (as indicated), the cells on the underside of the membrane were fixed, stained with "cristal violet," and counted by bright-field microscopy in 5 random fields (magnification: ×200). Bars, mean ± SD of at least 3 independent experiments carried out in duplicate (***, $P < 0.005$); right: photographs of representative random fields (magnification: ×200) of each group. C, top: zymography analysis of conditioned media from 48 hours serum-free cultures of HOS-P, -M, and -S7 cells treated with 5 ng/mL TGFβ or untreated. A Coomassie blue stained gel representative of 3 independent experiments is shown; bottom: zymography analysis of conditioned media from 48 hours serum-free cultures of HOS cells treated with 5 ng/mL TGFβ in the presence or absence of SD-208 (10 μmol/L). A Coomassie blue stained gel representative of 3 independent experiments is shown. D, top: HOS-P, -M, and -S7 cells were incubated with TGFβ1 (5 ng/mL) for 24 hours (left). HOS cells were incubated with TGFβ1 (5 ng/mL) in the presence or absence of SD-208 (10 μmol/L) for 24 hours (right). After incubation, *MMP2* mRNA steady-state levels were determined by quantitative RT-PCR. Bars, mean ± SD of at least 3 independent experiments carried out in duplicate (*, $P < 0.05$; ***, $P < 0.005$). Bottom, RNA was extracted from tumor biopsies of mice injected with parental (black), mock- (gray), and Smad7- (white) transfected HOS cells (left). RNA was extracted from tumor biopsies of mice injected with HOS cells and treated with SD-208 at 20 mg/kg/day (gray), SD-208 at 60 mg/kg/day (white), or with vehicle (black; right). *MMP2* mRNA steady-state levels were determined by quantitative RT-PCR. Bars, mean ± SD of 2 independent experiments carried out in duplicate (*, $P < 0.05$).

Published OnlineFirst August 8, 2014; DOI: 10.1158/1078-0432.CCR-13-3191

development of primary bone tumors (37). Cancer cells produce soluble factors that activate directly or indirectly via osteoblasts, the osteoclast differentiation, and maturation (38, 39). In turn, during bone degradation, osteoclasts allow the release of growth factors stored in the mineralized bone matrix that are able to stimulate tumor growth. In this context, we demonstrated that the resulting increase in bone volume observed after Smad7 overexpression in osteosarcoma cells is due in large part to the inhibition of osteoclast activity. The decrease of TRAP activity at the growth plate level, which is not in direct contact with the tumor, suggests that Smad7 overexpression affects the ability of the tumor cells to produce a soluble factor able to regulate osteoclast activity. Here, we clearly demonstrated that Smad7 overexpression in osteosarcoma cells inhibits their ability to produce RANKL or IL11, 2 cytokines that play a central role in bone osteolysis process (40). Together, these results suggest that Smad7 slows the tumor growth by acting at least at the tumor environment level, by inhibiting the tumor associated bone osteolysis.

Surprisingly, we did not observe a significant effect of SD-208 on tumor growth. Several hypotheses can be proposed to explain this difference between Smad7 and SD-208 effects on tumor growth. First, we cannot rule out that Smad7 may also exert some of its action independently from its role as a TGFβ signaling inhibitor. Indeed, Smad7 is able to inhibit other signaling pathways such as the cascade of bone morphogenetic protein family members (BMP), highly involved in bone formation (41). This hypothesis seems unlikely because the BMPs are known to promote bone formation. Thus, we can hypothesize that BMP inhibitors should promote bone degradation by inhibiting the bone formation in contrast to the results observed by overexpression of Smad7. Second, Smad7 might have several distinct functions in cellular signaling (12). For example it has been shown that Smad7 overexpression is able to potentiate apoptosis in prostate carcinoma and in PC-3U cells (12). In addition, Smad7 is also able to activate some signaling pathways such as the JNK cascade (42). Although we have not observed an effect of Smad7 on the proliferation and apoptosis of osteosarcoma cells, or on the ability of TGFβ to stimulate the MAPK pathway, we cannot rule out this hypothesis. Third, the inefficiency of SD-208 on tumor growth can be explained by its inability to reduce the tumor-associated bone osteolysis. Indeed, although a systemic treatment of mice with SD-208 promotes bone formation in absence of tumor as previously described (30), this systemic treatment does not seem to reduce the tumor associated bone osteolysis in contrast with the overexpression of Smad7 effect in osteosarcoma cells. In addition, the HOS mice model used in these experiments is a high aggressive model with a fast bone degradation associated with tumor growth. The effectiveness of a local mice treatment with SD-208 directly into the tumor cells using a less aggressive model should be tested.

Finally, we showed that both Smad7 overexpression and SD-208 strongly affect the ability of the primary bone tumor to develop lung metastasis, demonstrating the crucial role of TGFβ/Smad signaling pathway in the metastatic process of osteosarcoma. During the last decades, the role of TGFβ in the metastatic process of carcinomas has been widely described. A major step in this process is the ability of TGFβ to stimulate epithelial-to-mesenchymal transition and thus the ability of tumor cells to invade adjacent tissues (17). In the context of osteosarcoma cells that are from mesenchymal origin, we specifically demonstrated that Smad7 overexpression and SD-208 block the ability of TGFβ to stimulate osteosarcoma migration and invasion. In this context, we clearly demonstrated that Smad7 and SD-208 are able to block TGFβ-induced MMP2 activity, mainly involved in the invasion process such as described in the context of melanoma bone metastasis (19, 20). Another major step in the metastatic process is the ability of TGFβ to stimulate tumor-associated angiogenesis and thus the dissemination of tumor cells into the bloodstream (17). In this context, we clearly demonstrated that both Smad7 and SD-208 reduce the angiogenic process as shown by immunohistochemical staining for the endothelial marker CD146. In addition, both Smad7 and SD-208 inhibit TGFβ-induced *VEGF* expression, mainly involved in the angiogenic process. Moreover, both Smad7 and SD-208 are able to inhibit the ability of TGFβ to stimulate the expression of *ANGPLT4* and *CXCR4* identified as key players to prime breast cancer cells for metastasis respectively toward the lungs (43) and toward the bones or the lungs (44).

In conclusion, this report provides evidence that blocking TGFβ signaling may represent a novel therapeutic approach to treat lung metastasis in patients with osteosarcoma, which have a poor prognosis.

Disclosure of Potential Conflicts of Interest

No potential conflicts of interest were disclosed.

Authors' Contributions

Conception and design: A. Lamora, F. Redini, F. Verrecchia
Development of methodology: A. Lamora, J. Talbot, G. Bougras, J. Amiaud, M. Leduc, J. Chesneau, F. Verrecchia
Acquisition of data (provided animals, acquired and managed patients, provided facilities, etc.): A. Lamora, M.C. Le Deley, M.F. Heymann, F. Verrecchia
Analysis and interpretation of data (e.g., statistical analysis, biostatistics, computational analysis): A. Lamora, J. Talbot, J. Amiaud, M. Leduc, J. Chesneau, D. Heymann, F. Redini, F. Verrecchia
Writing, review, and/or revision of the manuscript: A. Lamora, V. Stresing, D. Heymann, F. Redini, F. Verrecchia
Administrative, technical, or material support (i.e., reporting or organizing data, constructing databases): A. Lamora, J. Talbot, J. Amiaud, M. Leduc, J. Chesneau, J. Taurelle, F. Verrecchia
Study supervision: A. Lamora, M.C. Le Deley, M.F. Heymann, F. Verrecchia

Acknowledgments

The authors thank Nicolas Pelletier, Arnaud Tessier, and Jacques Lebreton (CEISAM UMR6230, Nantes University, France) for the synthesis of SD-208.

Published OnlineFirst August 8, 2014; DOI: 10.1158/1078-0432.CCR-13-3191

Grant Support

This work was supported by INSERM, Ligue contre le Cancer (Allocation doctorale to A. Lamora), Ligue contre le Cancer (Equipe labellisée 2012), and Fondation Bettencourt Schueller.

The costs of publication of this article were defrayed in part by the payment of page charges. This article must therefore be hereby marked *advertisement* in accordance with 18 U.S.C. Section 1734 solely to indicate this fact.

Received November 28, 2013; revised July 8, 2014; accepted July 18, 2014; published OnlineFirst August 8, 2014.

References

1. Mirabello L, Troisi RJ, Savage SA. International osteosarcoma incidence patterns in children and adolescents, middle ages and elderly persons. Int J Cancer 2009;125:229–34.
2. Broadhead ML, Clark JCM, Myers DE, Dass CR, Choong PFM. The molecular pathogenesis of osteosarcoma: a review. Sarcoma 2011; 2011:1–12.
3. Yarber JL, Agulnik M. Targeted therapies in bone sarcomas: current approach and future directions. Expert Opin Investig Drugs 2011; 20:973–9.
4. Meyers PA, Gorlick R. Osteosarcoma. Pediatr Clin North Am 1997; 44:973–89.
5. Hughes DPM. Strategies for the targeted delivery of therapeutics for osteosarcoma. Expert Opin Drug Deliv 2009;6:1311–21.
6. Anninga JK, Gelderblom H, Fiocco M, Kroep JR, Taminiau AHM, Hogendoorn PCW, et al. Chemotherapeutic adjuvant treatment for osteosarcoma: where do we stand? Eur J Cancer 2011;47: 2431–45.
7. Ando K, Mori K, Corradini N, Redini F, Heymann D. Mifamurtide for the treatment of nonmetastatic osteosarcoma. Expert Opin Pharmacother 2011;12:285–92.
8. PosthumaDeBoer J, Witlox MA, Kaspers GJL, van Royen BJ. Molecular alterations as target for therapy in metastatic osteosarcoma: a review of literature. Clin Exp Metastasis 2011;28: 493–503.
9. Eccles SA, Welch DR. Metastasis: recent discoveries and novel treatment strategies. Lancet 2007;369:1742–57.
10. Feng X-H, Derynck R. Specificity and versatility in TGF-β signaling through Smads. Annu Rev Cell Dev Biol 2005;21:659–93.
11. Shi Y, Massagué J. Mechanisms of TGF-β signaling from cell membrane to the nucleus. Cell 2003;113:685–700.
12. Park SH. Fine tuning and cross-talking of TGF-β signal by inhibitory Smads. J Biochem Mol Biol 2005;38:9–16.
13. Katsuno Y, Lamouille S, Derynck R. TGF-β signaling and epithelial-mesenchymal transition in cancer progression. Curr Opin Oncol 2013;25:76–84.
14. Nakao A, Afrakhte M, Morén A, Nakayama T, Christian JL, Heuchel R, et al. Identification of Smad7, a TGF-β-inducible antagonist of TGF-β signalling. Nature 1997;389:631–5.
15. Hayashi H, Abdollah S, Qiu Y, Cai J, Xu YY, Grinnell BW, et al. The MAD-related protein Smad7 associates with the TGF-β receptor and functions as an antagonist of TGF-β signaling. Cell 1997; 89:1165–73.
16. Verrecchia F, Mauviel A, Farge D. Transforming growth factor-β signaling through the Smad proteins: role in systemic sclerosis. Autoimmun Rev 2006;5:563–9.
17. Meulmeester E, Ten Dijke P. The dynamic roles of TGF-β in cancer. J Pathol 2011;223:205–18.
18. Yin JJ, Selander K, Chirgwin JM, Dallas M, Grubbs BG, Wieser R, et al. TGF-β signaling blockade inhibits PTHrP secretion by breast cancer cells and bone metastases development. J Clin Invest 1999;103: 197–206.
19. Javelaud D, Delmas V, Möller M, Sextius P, André J, Menashi S, et al. Stable overexpression of Smad7 in human melanoma cells inhibits their tumorigenicity *in vitro* and *in vivo*. Oncogene 2005; 24:7624–9.
20. Javelaud D, Mohammad KS, McKenna CR, Fournier P, Luciani F, Niewolna M, et al. Stable overexpression of Smad7 in human melanoma cells impairs bone metastasis. Cancer Res 2007;67: 2317–24.
21. Mohammad KS, Javelaud D, Fournier PGJ, Niewolna M, McKenna CR, Peng XH, et al. TGF-β-RI kinase inhibitor SD-208 reduces the development and progression of melanoma bone metastases. Cancer Res 2011;71:175–84.
22. Mundy GR. Metastasis to bone: causes, consequences and therapeutic opportunities. Nat Rev Cancer 2002;2:584–93.
23. Kozlow W, Guise TA. Breast cancer metastasis to bone: mechanisms of osteolysis and implications for therapy. J Mammary Gland Biol Neoplasia 2005;10:169–80.
24. Franchi A, Arganini L, Baroni G, Calzolari A, Capanna R, Campanacci D, et al. Expression of transforming growth factor-β isoforms in osteosarcoma variants: association of TGF-β1 with high-grade osteosarcomas. J Pathol 1998;185:284–9.
25. Mohseny AB, Cai Y, Kuijjer M, Xiao W, van den Akker B, de Andrea CE, et al. The activities of Smad and Gli mediated signalling pathways in high-grade conventional osteosarcoma. Eur J Cancer Oxf Engl 1990 2012;48:3429–38.
26. Matsuyama S, Iwadate M, Kondo M, Saitoh M, Hanyu A, Shimizu K, et al. SB-431542 and Gleevec inhibit transforming growth factor-β-induced proliferation of human osteosarcoma cells. Cancer Res 2003;63:7791–8.
27. Talbot J, Brion R, Picarda G, Amiaud J, Chesneau J, Bougras G, et al. Loss of connexin43 expression in Ewing's sarcoma cells favors the development of the primary tumor and the associated bone osteolysis. Biochim Biophys Acta 2013;1832:553–64.
28. Dennler S, Itoh S, Vivien D, ten Dijke P, Huet S, Gauthier JM. Direct binding of Smad3 and Smad4 to critical TGF-β-inducible elements in the promoter of human plasminogen activator inhibitor-type 1 gene. EMBO J 1998;17:3091–100.
29. Heymann D, Ory B, Blanchard F, Heymann M-F, Coipeau P, Charrier C, et al. Enhanced tumor regression and tissue repair when zoledronic acid is combined with ifosfamide in rat osteosarcoma. Bone 2005; 37:74–86.
30. Mohammad KS, Chen CG, Balooch G, Stebbins E, McKenna CR, Davis H, et al. Pharmacologic inhibition of the TGF-β type I receptor kinase has anabolic and anti-catabolic effects on bone. PLoS ONE 2009;4:e5275.
31. Levy L, Hill CS. Alterations in components of the TGF-β superfamily signaling pathways in human cancer. Cytokine Growth Factor Rev 2006;17:41–58.
32. Dalal BI, Keown PA, Greenberg AH. Immunocytochemical localization of secreted transforming growth factor-β1 to the advancing edges of primary tumors and to lymph node metastases of human mammary carcinoma. Am J Pathol 1993;143:381–9.
33. Tsushima H, Kawata S, Tamura S, Ito N, Shirai Y, Kiso S, et al. High levels of transforming growth factor-β1 in patients with colorectal cancer: association with disease progression. Gastroenterology 1996; 110:375–82.
34. Wikström P, Stattin P, Franck-Lissbrant I, Damber JE, Bergh A. Transforming growth factor-β1 is associated with angiogenesis, metastasis, and poor clinical outcome in prostate cancer. Prostate 1998;37:19–29.
35. Pfeilschifter J, D'Souza SM, Mundy GR. Effects of transforming growth factor-β on osteoblastic osteosarcoma cells. Endocrinology 1987; 121:212–8.
36. Kloen P, Jennings CL, Gebhardt MC, Springfield DS, Mankin HJ. Expression of transforming growth factor-β (TGF-β) receptors, TGF-β1 and TGF-β2 production and autocrine growth control in osteosarcoma cells. Int J Cancer 1994;58:440–5.
37. Halvorson KG, Sevcik MA, Ghilardi JR, Rosol TJ, Mantyh PW. Similarities and differences in tumor growth, skeletal remodeling and pain in an osteolytic and osteoblastic model of bone cancer. Clin J Pain 2006;22:587–600.

Published OnlineFirst August 8, 2014; DOI: 10.1158/1078-0432.CCR-13-3191

38. Guise TA, Yin JJ, Taylor SD, Kumagai Y, Dallas M, Boyce BF, et al. Evidence for a causal role of parathyroid hormone-related protein in the pathogenesis of human breast cancer-mediated osteolysis. J Clin Invest 1996;98:1544–9.
39. Grano M, Mori G, Minielli V, Cantatore FP, Colucci S, Zallone AZ. Breast cancer cell line MDA-231 stimulates osteoclastogenesis and bone resorption in human osteoclasts. Biochem Biophys Res Commun 2000;270:1097–100.
40. Boyle WJ, Simonet WS, Lacey DL. Osteoclast differentiation and activation. Nature 2003;423:337–42.
41. Mochizuki T, Miyazaki H, Hara T, Furuya T, Imamura T, Watabe T, et al. Roles for the MH2 domain of Smad7 in the specific inhibition of transforming growth factor-β superfamily signaling. J Biol Chem 2004;279:31568–74.
42. Mazars A, Lallemand F, Prunier C, Marais J, Ferrand N, Pessah M, et al. Evidence for a role of the JNK cascade in Smad7-mediated apoptosis. J Biol Chem 2001;276:36797–803.
43. Padua D, Zhang XH-F, Wang Q, Nadal C, Gerald WL, Gomis RR, et al. TGFβ primes breast tumors for lung metastasis seeding through angiopoietin-like 4. Cell 2008;133:66–77.
44. Liang Z, Wu T, Lou H, Yu X, Taichman RS, Lau SK, et al. Inhibition of breast cancer metastasis by selective synthetic polypeptide against CXCR4. Cancer Res 2004;64:4302–8.

Published OnlineFirst August 8, 2014; DOI: 10.1158/1078-0432.CCR-13-3191

Clinical Cancer Research

Overexpression of Smad7 Blocks Primary Tumor Growth and Lung Metastasis Development in Osteosarcoma

Audrey Lamora, Julie Talbot, Gwenola Bougras, et al.

Clin Cancer Res 2014;20:5097-5112. Published OnlineFirst August 8, 2014.